Three-Dimensional Visualization of the Interaction between a Vortex Ring and a Stratified Interface: The Evolution of the Density Field

Jason Olsthoorn, and Stuart B. Dalziel

Department of Applied Mathematics and Theoretical Physics, University of Cambridge, Centre for Mathematical Sciences, Wilberforce Road, Cambridge UK, CB3 0WA
jo344@cam.ac.uk

Abstract

The study of vortex-ring-induced stratified mixing has long played a key role in understanding externally-forced, stratified turbulent mixing. While several studies have investigated the dynamical evolution of a such a stratified system, this paper presents an experimental investigation of the three-dimensional mechanical evolution of these vortex rings with the specific goal of a understanding how vortex rings induce mixing of the density field.

Through the use of modern imaging techniques, we reconstruct a full, three-dimensional, time-resolved velocity field encapsulating the interaction of a vortex ring with a stratified interface. Using a numerical scheme, we back out the density field from the experimentally determined velocity field. This work agrees with many of the previous two-dimensional studies, while capturing the three-dimensional instabilities of the system. The horizontally-averaged vertical buoyancy flux is then presented as a function of time which helps to explain the interface sharpening observed elsewhere.

1 Introduction

Vortex-ring-induced stratified mixing was originally investigated in Linden (1973), which presented a theoretical prediction for the entrainment rate of individual vortex rings. Since that time, many studies (See Fernando (1991) and the references therein) have observed similar entrainment scaling laws in the context of turbulent mixing. Indeed, Linden is still cited as one of the canonical entrainment rate results (Shrinivas and Hunt, 2015). Forty-three years later, our ability to observe and quantify the vortex-ring-induced mixing has drastically improved. Indeed, Olsthoorn and Dalziel (2015) recently challenged the Linden scaling by re-investigating the mixing induced by a large number of vortex rings in a stratified fluid. As with vortex-ring-induced mixing, understanding the mechanics of the vortex-ring interaction will play a key role in understanding how mixing occurs in a stratified turbulence context.

One of the key features of stratified turbulent mixing is the formation of layers (Park et al., 1994; Oglethorpe et al., 2013). In fact, Phillips (1972) and Posmentier (1977) have proposed one theoretical argument of how layers form based upon the bulk entrainment dynamics of the system. However, the mechanics of layer formation remains elusive. It has been shown that vortex rings sharpen density interfaces during their interaction (Olsthoorn and Dalziel, 2015). Understanding how vortex rings establish sharp layers may help highlight the mechanism of layer formation in stratified turbulence.

This paper presents the three-dimensional visualization of a vortex ring impacting on a stratified interface. Here, only one parameter case will be presented. We will show that there is a distinct asymmetric nature to the buoyancy flux produced by the vortex-ring interaction which will result in the sharpening of the density interface.

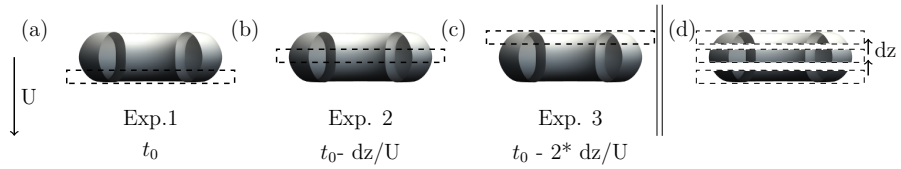

Figure 1: Diagram of the velocity-reconstruction process, highlighting the change in horizontal light sheet.

2 Methods

In a recently submitted paper, Olsthoorn and Dalziel (Submitted) present time-resolved experimental velocity-field measurements of a vortex ring interacting with a stratified interface within a three-dimensional domain. We will not reproduce that discussion here, but rather, we will give a brief overview of the methodology. We encourage reader to refer to the cited paper for more details.

In a tank ($0.45 \times 0.45 \times 0.60$ m^3), a two-layer stratification was established. The two fluid layers were refractive-index matched using a combination of sodium chloride and sodium nitrate solutions (McDougall, 1979). Within the tank, a downward propagating vortex ring was generated at the top of the water column. The vortex rings were produced using a computer controlled pressure pulse, as described in Olsthoorn and Dalziel (2015). Using a horizontal laser sheet, the authors measured the three-components of velocity of the vortex-ring interaction within a single plane. The position of the density interface was then shifted by removing fluid from the base of the tank, effectively moving the position of the light sheet relative to the stratification. Thus, by producing a subsequent vortex ring, the authors measured the velocity field of the vortex-ring interaction on a different horizontal plane. By iterating this procedure, they produce a sequence of velocity slices, which, when appropriately time correlated and filtered, produce an ensemble capturing the reproducible components of the vortex-ring interaction. A diagram of this process is provided in figure 4. The density field during the interaction was not experimentally measured in this process.

By inputting this velocity field ensemble into an in-house third-order pseudospectral advection-diffusion-equation solver, we numerically compute the evolution of the density field. Specifically, given the velocity field ensemble ($\vec{u}_E$) computed as above, the density field is given by:

$$\partial_t \rho + \vec{u}_E \cdot \nabla \rho = \kappa \nabla^2 \rho, \qquad \rho(t=0) = \frac{\Delta\rho}{2}\left(1 + \tanh\left[\frac{z - z_\rho}{\sigma}\right]\right). \tag{1}$$

The molecular diffusion coefficient was set to $\kappa = 1 \times 10^{-6}$ m^2/s, equal to the molecular viscosity of water. This choice of κ is significantly larger than the experimental salt-water value but is sufficient for our purposes here. The value of the density difference between the two layers ($\Delta\rho$) does not affect the structure of the results due to the linearity of equation (1). The position (z_ρ) and width (σ) of the density interface were estimated from the computed displacement of Lagrangian particles, not shown here. A filter was applied to remove spectral aliasing. For technical reasons, the density field could not be measured directly during this ensemble of experiments.

The vortex-ring interaction can be characterized by two dimensionless parameters: the Reynolds number (Re) of the vortex ring and the bulk Richardson number (Ri) of the stratification. For the vortex-ring interaction presented here, the vortex ring's velocity

($U = 0.061$ m/s) and vortex-tube diameter ($D = 0.039$ m) characterize the vortex ring. Thus,

$$\mathrm{Re} = \frac{UD}{\nu} = 2400, \qquad \mathrm{Ri} = \frac{g\Delta\rho}{\rho_0}\frac{D}{U^2} = 1.7.$$

Here, $\nu = 10^{-6}$ m^2/s is the molecular viscosity of water, g is the acceleration due to gravity and $\rho_0 = 1 \times 10^{-3}$ kg/ m^3 is the reference density of fresh water. The density jump across the interface was $\Delta\rho = 1.7 \times 10^{-5}$ kg/ m^3. For the remainder of this discussion, all length scales have been non-dimensionalized by D and time has been non-dimensionalized by the advective timescale $t^* = \frac{D}{U}$. Density has also be non-dimensionalized by the top-to-bottom density difference.

3 Results

Figure 2 plots the evolution of the vorticity and density field of the vortex-ring interaction at non-dimensional time $t = 0$ (a)-(b), $t = 1$ (c)-(d), $t = 2$ (e)-(f), and $t = 3$ (g)-(h). Note that the time of the first panel has been arbitrarily chosen to be $t = 0$. Both the vorticity and density field have been sliced through the vortex ring's centre in order to visualize the core dynamics. This figure plots the vortex ring as it approaches the density interface (panels (a)-(b)), where the interface depresses in the presence of the vortex ring's associated velocity field. As the density field is deformed, the baroclinic shear will produce vorticity of the opposite sign (red) to the impinging vortex ring (blue) (panels (c)-(d)). As time progresses (panels (e)-(f)), this baroclinic vorticity transfer (BVT) will 'unwind' the vortex ring. The BVT produced vorticity will entrain lower layer fluid into the upper layer where the mass diffusion necessary for mixing will occur. As this vortex ring has sufficient energy to penetrate into the lower layer, the lateral buoyancy gradient will compress the vortex ring (see panels (g)-(h)) until the it has been sufficiently eroded, at which point the interface will rebound, further ejecting fluid into the upper layer.

In order to verify the present methodology, the three-dimensional ensemble generated using a horizontal light sheet was compared with the measurements of a vortex-ring interaction (Re= 2400, Ri= 1.8) obtained using a vertical light sheet. In contrast to a horizontal light sheet, a vertical light sheet provides us with density and velocity field measurements from a single experiment at the expense of the three-dimensional information of the interaction. Figure 3 compares the results of a vertical light sheet (panels (a)-(c)) with the computed three-dimensional density and velocity field (panels (b)-(d) respectively.) We see that there is a very good agreement between the directly observed density field (a) and the ensemble determined density field (b). There exists strong quantitative agreement between the vorticity field computed using a vertical light sheet (c), and the reconstructed vorticity field (d) (both plots have the same colour saturation). The agreement between these two approaches provides a validation of the current computational methodology.

The purpose of this discussion is to investigate the interface sharpening observed experimentally (Olsthoorn and Dalziel, 2015). One measure of the local increase in the potential energy of the system is the vertical buoyancy flux. We note that this buoyancy flux is not a measure of true mixing (resulting from an irreversible change in potential energy) as it includes the reversible change in the potential energy of the system, that is, the available potential energy. However, the buoyancy flux does provide a measure for the 'stirring' of the stratification. Thus, figure 4 plots the horizontally-averaged vertical buoyancy flux ($< \rho w >$, where the angled brackets denote a horizontal average) as a

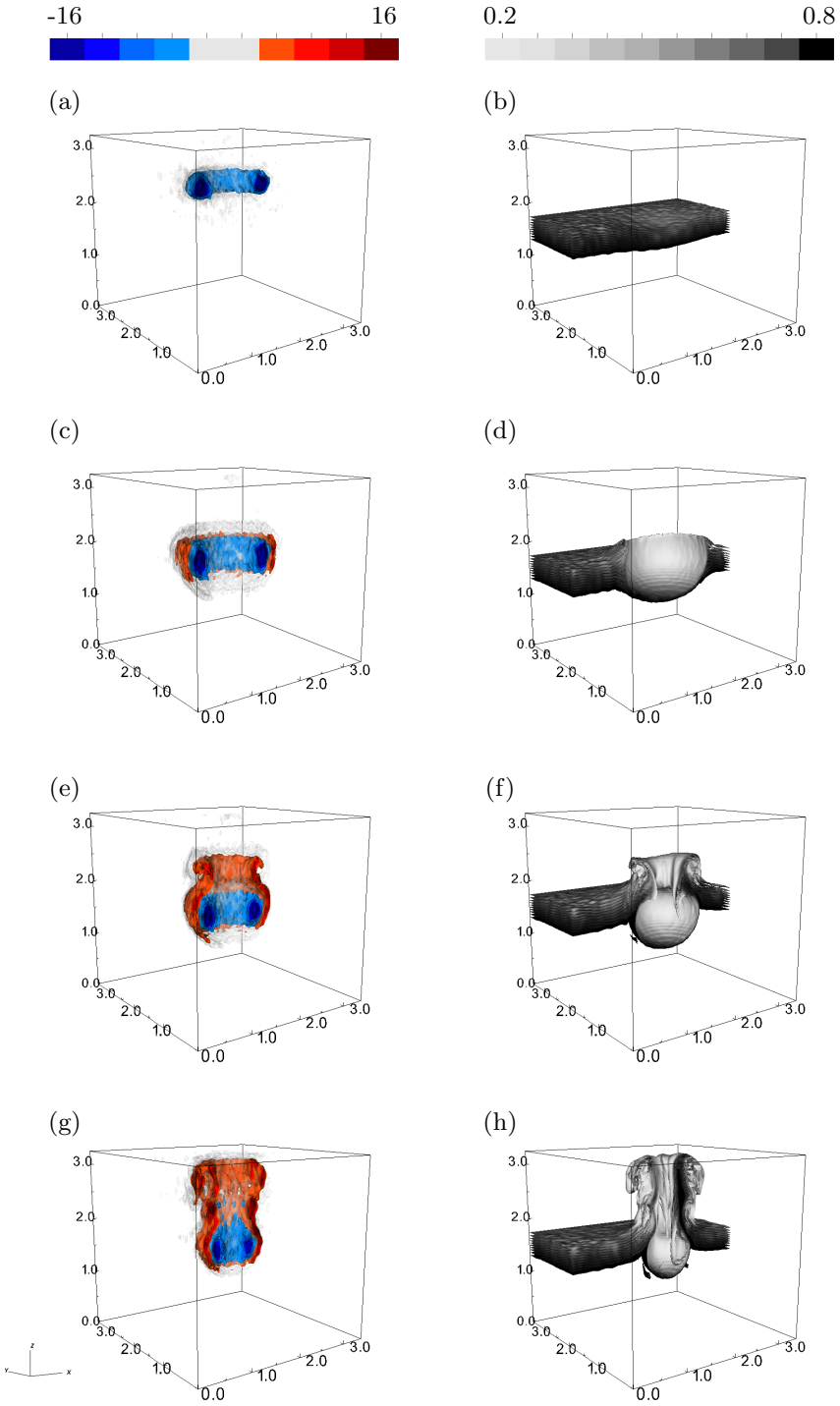

Figure 2: Plot of the evolution of the vortex-ring interaction over time. Panels (a),(c),(e),(g) plot the azimuthal vorticity and panels (b),(d),(f),(h) plot the evolution of the computed density field. Panels have been plot at t = 0 (a)-(b), t=1 (c)-(d), t=2 (e)-(f), t=3(g)-(h). Both vorticity and density are presented in non-dimensional units.

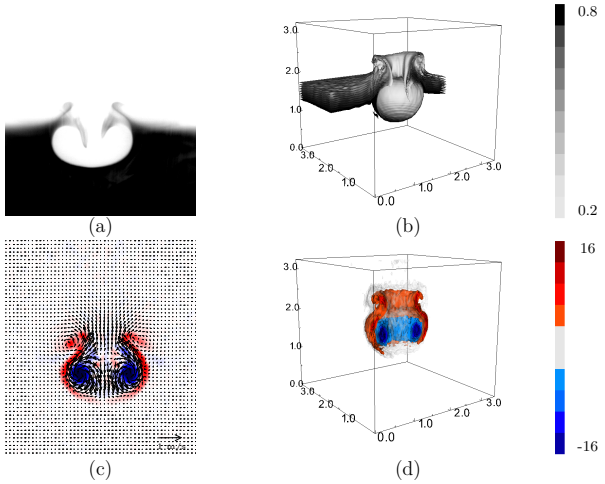

Figure 3: Comparison between the density (panels (a)-(b)) and vorticity (panels (c)-(d)) measurements observed using two different light-sheet orientations. Panels (a),(c) are computed from a vertical light sheet, whereas panels (b),(d) are computed from a horizontal light sheet using the layering methodology. Note that the colour scheme of panel (c) was inverted across the vortex ring's central axis in order to make the comparison with panel (d).

function of time. The key feature-of-note in this plot is the location of the peak in vertical buoyancy flux, ($t \sim 5$). We observe that the dominant buoyancy flux occurs above the equilibrium height of the interface (plotted as a solid line). Indeed, this peak in buoyancy flux is approximately four times larger than the negative buoyancy flux produced during the impingement of the vortex ring. The asymmetric buoyancy flux about the interface was noted previously when discussing figure 2 but, figure 4 provides a quantified metric indicating that the vertical buoyancy flux is predominantly positive and above the density interface. This asymmetry in the vertical buoyancy flux explains why the interface sharpens over subsequent vortex-ring interactions.

4 Conclusions

We present the three-dimensional visualization of an experimental vortex ring as it impacts onto a stratified interface. In particular, we highlight how the density field evolves during this interaction. The results presented above provide a quantitative explanation of why the interaction of a vortex ring with a density stratification sharpens interfaces. This asymmetric mixing of buoyancy has also been suggested by Camassa et al. (2013). Futher work is required to show how the buoyancy flux and mixing change as a function of Reynolds and Richardson number.

5 Acknowledgments

Support for this work was provided by the Natural Sciences and Engineering Research Council of Canada (NSERC) and through the Engineering and Physical Sciences Research Council (EPSRC) grant number EP/L504920/1. Additional support has been provided by the EPSRC Mathematical Underpinnings of Stratified Turbulence grant XXXXXXXXX.

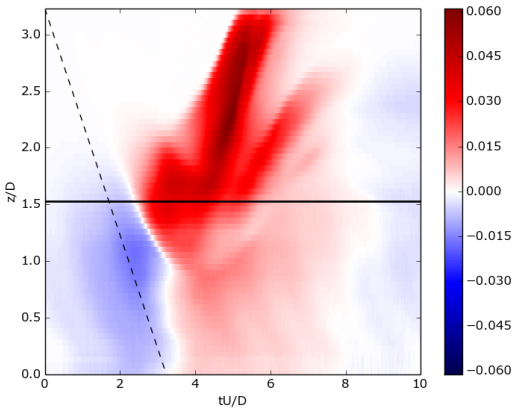

Figure 4: Plot of the horizontally averaged vertical buoyancy flux as a function of time. A horizontal line has been plotted at the equilibrium height of the density interface. The dashed line plots a representative trajectory for the vortex ring in the absense of the stratification.

References

Camassa, R., Khatri, S., McLaughlin, R., Mertens, K., Nenon, D., Smith, C., and Viotti, C. (2013). Numerical simulations and experimental measurements of dense-core vortex rings in a sharply stratified environment. *Computational Science & Discovery*, 6(1):014001.

Fernando, H. J. S. (1991). Turbulent mixing in stratified fluids. *Annual Review of Fluid Mechanics*, 23(1):455–493.

Linden, P. F. (1973). The interaction of a vortex ring with a sharp density interface: a model for turbulent entrainment. *Journal of Fluid Mechanics*, 60:467–480.

McDougall, T. J. (1979). On the elimination of refractive-index variations in turbulent density-stratified liquid flows. *Journal of Fluid Mechanics*, 93:83–96.

Oglethorpe, R. L. F., Caulfield, C. P., and Woods, A. W. (2013). Spontaneous layering in stratified turbulent taylorcouette flow. *Journal of Fluid Mechanics*, 721:R3, 1–12.

Olsthoorn, J. and Dalziel, S. B. (2015). Vortex-ring-induced stratified mixing. *Journal of Fluid Mechanics*, 781:113–126.

Olsthoorn, J. and Dalziel, S. B. (Submitted). Three-dimensional visualization of vortex-ring interactions with a stratified interface. *Journal of Fluid Mechanics*.

Park, Y.-G., Whitehead, J. A., and Gnanadeskian, A. (1994). Turbulent mixing in stratified fluids: layer formation and energetics. *Journal of Fluid Mechanics*, 279:279–311.

Phillips, O. (1972). Turbulence in a strongly stratified fluidis it unstable? *Deep Sea Research and Oceanographic Abstracts*, 19(1):79 – 81.

Posmentier, E. S. (1977). The generation of salinity finestructure by vertical diffusion. *Journal of Physical Oceanography*, 7(2):298–300.

Shrinivas, A. B. and Hunt, G. R. (2015). Confined turbulent entrainment across density interfaces. *Journal of Fluid Mechanics*, 779:116–143.